

LT $\alpha$ -deficient or -sufficient mice and mixed with BM cells from ROR $\gamma$ t-deficient mice into lethally irradiated recipients. F-ECs and *Fut2* expression were diminished in recipient mice reconstituted with BM cells containing LT $\alpha$ -deficient ROR $\gamma$ t<sup>+</sup> ILC3, whereas substantial numbers of F-ECs, and *Fut2* expression, were induced in recipient mice reconstituted with BM cells containing LT $\alpha$ -sufficient ROR $\gamma$ t<sup>+</sup> ILC3, indicating the importance of LT $\alpha$  expressed by ILC3 in the induction of F-ECs (Fig. 5, F to H). When the microbiota of LT $\alpha$ -deficient mice or of mixed BM chimeras containing LT $\alpha$ -deficient ILC3 were examined, substantial numbers of SFB were observed (fig. S6, A and B). From these results, we concluded that induction and maintenance of F-ECs were also regulated by ILC3-derived LT in a commensal flora-independent manner.

### Epithelial fucosylation protects against infection by *Salmonella typhimurium*

We next investigated the physiological role of epithelial fucosylation. With exception of Paneth

cells, the *Fut2* expression and ileal epithelial fucosylation observed in wild-type mice were abolished in *Fut2*<sup>-/-</sup> mice (fig. S11, A to E). We did not detect any overt changes in mucosal leukocyte populations or in IL-22 or LT expression in ILC3 in these mice (fig. S11F and table S1). Epithelial fucosylation provides an environmental platform for colonization by *Bacteroides* species (6–9); however, it is unknown whether epithelial fucosylation affects colonization and subsequent infection by pathogenic bacteria. To assess the effects of intestinal fucosylation on pathogenic bacterial infection, we first infected GF mice with the enteropathogenic bacterium *Salmonella typhimurium*, which has the potential to attach to fucose-containing carbohydrate molecules (42). After infection with *S. typhimurium*, ECs from both part 1 (duodenum) and part 4 (ileum) of the mouse intestine were fucosylated, and this was correlated with *Fut2* expression (Fig. 6, A and B). Previous reports have shown that expression of IL-22 in ILCs is much higher in mice infected with *S. typhimurium* (43, 44).

Therefore, *S. typhimurium*-induced epithelial fucosylation may be mediated by ILC3. Indeed, epithelial fucosylation was not induced in ROR $\gamma$ t-deficient mice after *S. typhimurium* infection (Fig. 6C). To investigate whether epithelial fucosylation has a role in regulating pathogenic bacterial infection, we infected wild-type or *Fut2*<sup>-/-</sup> mice with *S. typhimurium* and examined disease progression. Compared with wild-type mice, *Fut2*<sup>-/-</sup> mice were more susceptible to *Salmonella* infection accompanied with the observation of severe inflamed cecum (Fig. 6D). Consistent with the inflammatory status of diseased mice, the numbers of infiltrating leukocytes in cecum were higher in *Fut2*<sup>-/-</sup> mice than in wild-type mice (Fig. 6E). Although *S. typhimurium* titers in cecal contents were comparable between wild-type and *Fut2*<sup>-/-</sup> mice, increased numbers of *S. typhimurium* infiltrated the cecal tissue of *Fut2*<sup>-/-</sup> mice (Fig. 6F). These results suggest that epithelial fucosylation is dispensable for luminal colonization by *S. typhimurium* but inhibits bacterial invasion of intestinal

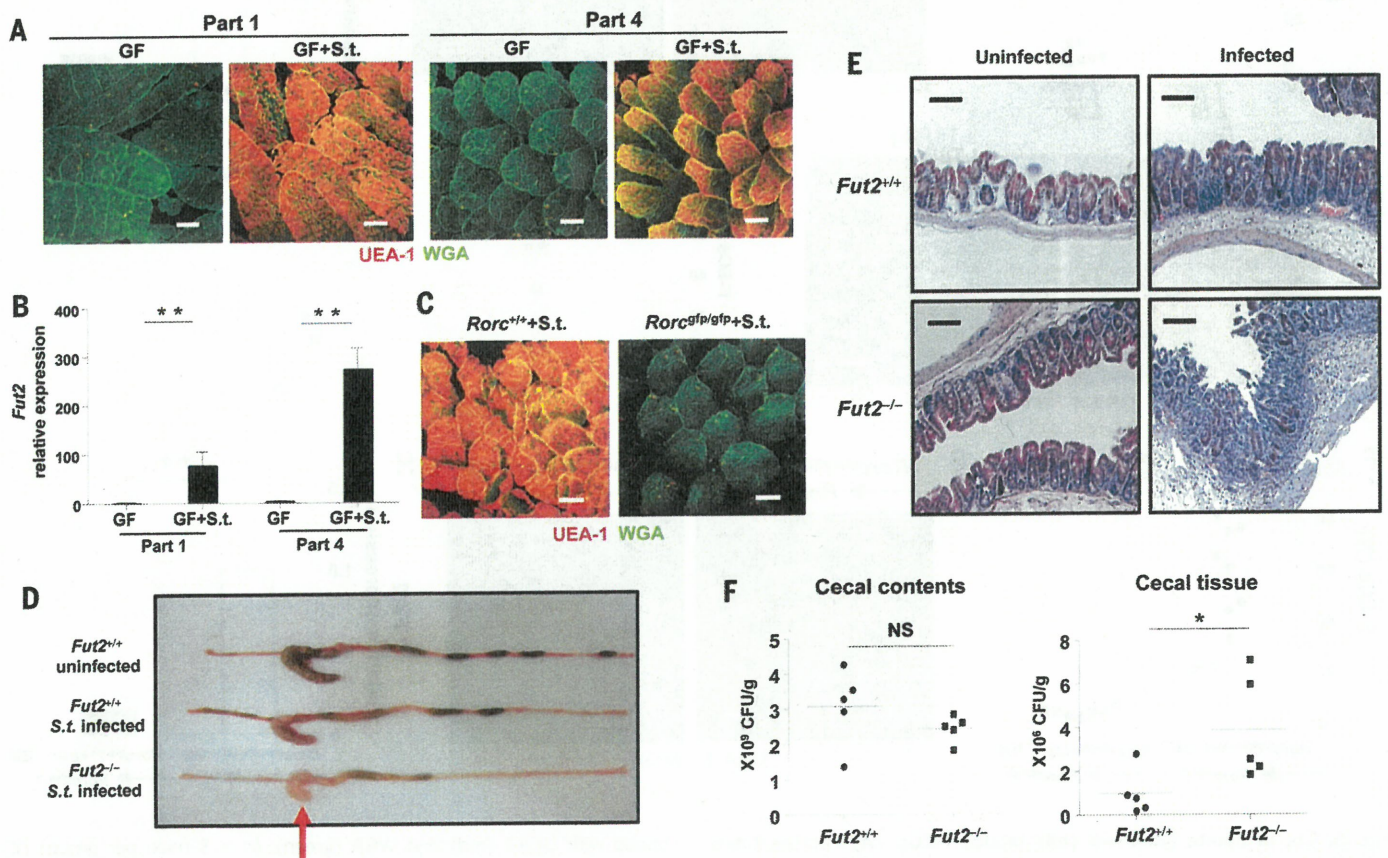


**Fig. 6. Epithelial fucosylation protects against infection by *S. typhimurium*.** (A) Whole-mount tissues from part 1 (duodenum) and part 4 (ileum) of the small intestines of germ-free (GF) or *S. typhimurium*-infected GF mice were stained with UEA-1 (red) and WGA (green) ( $n = 3$  to 4 mice per group). Scale bars, 100  $\mu$ m. (B) Epithelial *Fut2* expression in part 1 and part 4 of the small intestines of GF and *S. typhimurium*-infected GF mice was analyzed by using quantitative PCR ( $n = 3$  to 4 mice per group). Error bars indicate SD.  $***P < 0.01$  by using Student's *t* test. (C) Whole-mount tissues from ileum of *S. typhimurium*-infected *Rorc*<sup>+/+</sup> or *Rorc*<sup>GF/Grp</sup> mice were isolated and stained

with UEA-1 (red) and WGA (green) ( $n = 3$  to 4 mice per group). Scale bars, 100  $\mu$ m. (D and E) *Fut2*<sup>+/+</sup> or *Fut2*<sup>-/-</sup> mice were infected with *S. typhimurium*. Red arrow shows inflammation of the cecum. Representative macroscopic images (D) and hematoxylin and eosin-stained cecal sections (E) of infected or uninfected mice ( $n = 5$  mice per group). Scale bars, 100  $\mu$ m. (F) Numbers of bacteria in the luminal contents, and within the tissues, of the ceca of *Fut2*<sup>+/+</sup> or *Fut2*<sup>-/-</sup> mice were counted 24 hours after infection ( $n = 5$  mice per group).  $*P < 0.05$  by using Student's *t* test. NS, not significant. Three independent experiments were performed with similar results.

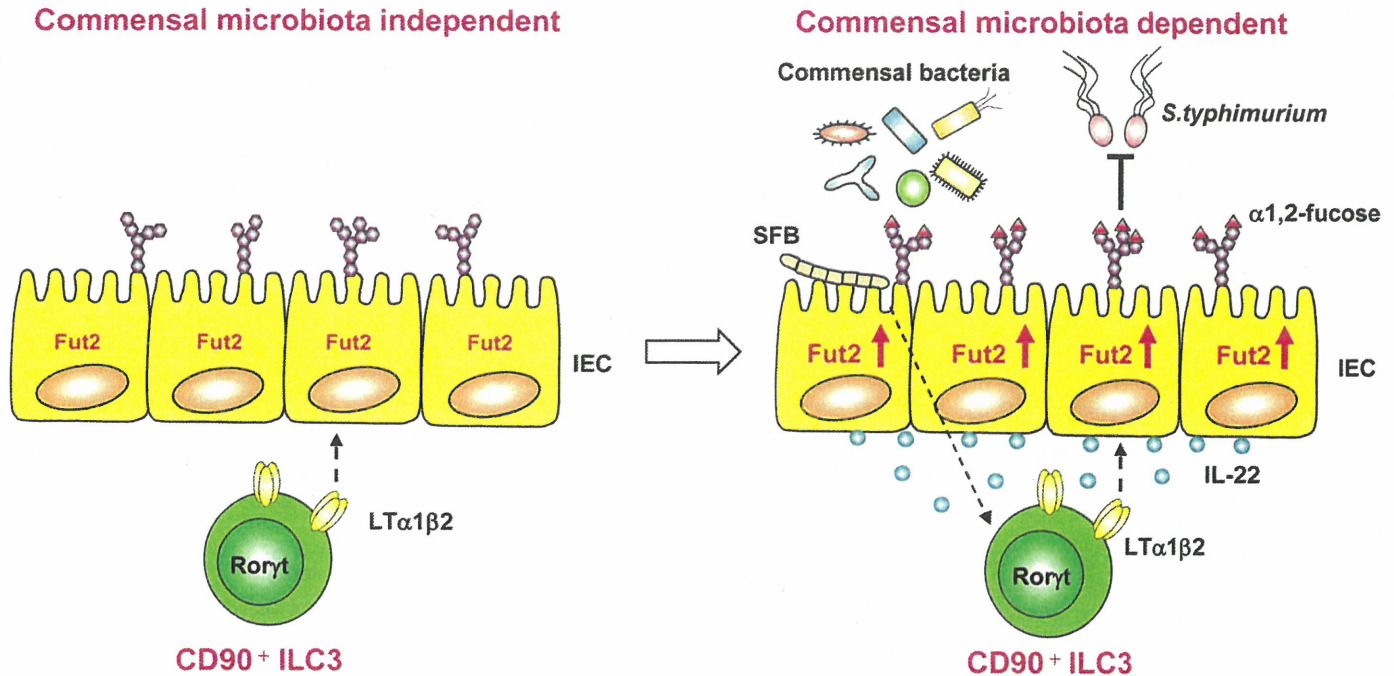


**Fig. 7. Scheme for the induction and regulation of epithelial fucosylation by ILC3.** IL-22<sup>-</sup> and LT $\alpha$ -producing ILC3 are critical cells for the induction and regulation of F-ECs. ILC3-mediated fucosylation of ECs is operated by commensal microbiota–dependent and –independent manners. Commensal bacteria, including SFB, stimulate CD90<sup>+</sup> ILC3 to produce IL-22 for the induction of Fut2 in ECs. On the other hand, LT $\alpha$  production by ILC3 are operated by a commensal bacteria–independent manner. ILC3-derived IL-22 and LT $\alpha$  induce Fut2 and subsequent epithelial fucosylation, which inhibits infection by *S. typhimurium*. IEC, intestinal epithelial cell.

tissues. Collectively, these results indicate that epithelial fucosylation, regulated by *Fut2*, has a protective role against infection by pathogenic bacteria.

## Discussion

The results of recent genome-wide association studies imply that *FUT2* nonsense polymorphisms affect the incidence of various metabolic and inflammatory diseases, including chronic intestinal inflammation such as Crohn's disease and infections with pathogenic microorganisms, especially Norwalk virus and rotavirus in humans (13–19). Understanding the mechanisms of regulation of *Fut2* gene expression and fucosylation, one of the major glycosylation events in intestinal ECs, is therefore of great interest. Previously, it was thought that epithelial fucosylation is initiated by direct interaction between commensals and ECs (7). Indeed, several reports have shown that epithelial fucosylation is actively induced and used by *Bacteroides* (8, 9). Here, we unexpectedly found that microbiota–epithelia cross-talk is insufficient to induce epithelial fucosylation, and rather, CD90<sup>+</sup> ROR $\gamma$ <sup>+</sup> ILC3 are necessary for induction of epithelial *Fut2* expression and consequent fucosylation. ILC3 located in the intestinal lamina propria express high levels of IL-22 in a commensal bacteria-dependent manner (Fig. 4I and fig. S7, A and D). This IL-22 then presumably binds to IL-22R expressed by intestinal ECs, leading to the induction of *Fut2* and initiation of the EC fucosylation process (Fig. 7). In contrast to the ex-

pression of IL-22, ILC3 express LT in a commensal bacteria–independent manner. Spontaneous expression of LT on ILC3 also contributes to the induction of epithelial fucosylation. To explain the mechanism underlying induction of epithelial fucosylation, we propose that epithelial fucosylation is regulated by a two-phase system orchestrated by ILC3 through the microbiota-independent production of LT and the induction of IL-22 by commensal bacteria (Fig. 7). Although other types of stimulation may also affect epithelial fucosylation, our findings reveal a critical role for ILC3.

Our results demonstrated that IL-22 produced by ILC3 is necessary and sufficient for induction of epithelial fucosylation when ILC3 are appropriately stimulated by commensal microbiota (Fig. 4, A to E). In addition to IL-22-mediated epithelial fucosylation, our results also show that the level of epithelial fucosylation is markedly reduced under LT $\alpha$ -deficient conditions (Fig. 5, A to C). Our findings suggest two possibilities for the IL-22/LT-mediated regulation of epithelial fucosylation. The first is that *Fut2* expression and subsequent epithelial fucosylation are induced when the intensity of synergistic or additive signals from IL-22 and LT is above the threshold for activation of *Fut2*. For example, LT produced by ILC3 provides the baseline signal for the minimum expression of *Fut2*, whereas commensal-mediated IL-22 produced by ILC3 drives the maximum expression of *Fut2* for the induction of epithelial fucosylation. The second possibility is that LT directly or indirectly regulates the expres-

sion of IL-22R by ECs, and vice versa, and/or the expression of IL-22. Indeed, a previous report has shown that LT produced by ILC3 regulates the expression of IL-23 by intestinal dendritic cells, as well as the subsequent production of IL-22 by ILC3 after infection with *C. rodentium* (45). How ILC3-derived IL-22 and LT regulate epithelial *Fut2* expression remains to be further elucidated.

Our findings provide further evidence of the critical roles of commensal microbiota, epithelial cells, and innate immune cells (such as ILC3) in the creation of a protective platform against infection by pathogenic bacteria (Fig. 7). Ablation of epithelial fucose allowed severe infection by the pathogenic bacteria *S. typhimurium* (Fig. 6, D to F). Although the detailed mechanisms of why *Fut2*<sup>-/-</sup> mice are susceptible to *Salmonella* infection remain unknown, one possibility is that fucosylated mucin produced by goblet cells blocks the attachment of *S. typhimurium* to the epithelium. Commensal microbes continuously stimulated goblet cells to release fucosylated mucin into the intestinal lumen (Fig. 2C). Indeed, in a previous *in vitro* study, H-type 2 antigens, which are synthesized by *Fut2* in intestinal ECs, prevented the binding of *S. typhimurium* to fucosylated epithelia; this supports our present findings (42). Our findings suggest a protective role for ILC3-mediated mucus-associated fucosylated glycan against infection by pathogenic bacteria.

ILC3 play critical roles in regulation of immune responses during mucosal infection, especially

by producing IL-22, which promotes subsequent expression of the antimicrobial molecule RegIII $\gamma$  by ECs (4, 36, 45). In addition to this, our results describe a previously unknown biological role for ILC3 in the induction and maintenance of intestinal epithelial glycosylation, which leads to the creation of an antipathogenic bacterial platform in the intestine (Fig. 7). Furthermore, epithelial fucosylation contributes to the creation of a cohabitation niche for the establishment of normal commensal microbiota (20, 21). Thus, ILC3-mediated control of epithelial-surface glycosylation might represent a general strategy for regulating the gut microenvironment. Targeted modification of these mechanisms has the potential to provide novel approaches for the control of intestinal infection and inflammation.

## Materials and Methods

### Mice

C57BL/6 and BALB/c mice were purchased from CLEA Japan (Tokyo, Japan). *Fut2*<sup>-/-</sup> and *Il22*<sup>-/-</sup> mice (C57BL/6 background) were generated as described previously, and *Id2*<sup>-/-</sup> mice were kindly provided by Y. Yokota (33, 46, 47). *Fut2*<sup>-/-</sup> mice were crossed onto the BALB/c background for six generations. *Rag2*<sup>-/-</sup> mice were kindly provided by F. Alt. *Rag1*<sup>-/-</sup>; *Rorc*<sup>gfp/gfp</sup>, *Il6*<sup>-/-</sup>, *Lia*<sup>-/-</sup>, *Tcr $\beta$* <sup>-/-</sup>  $\delta$ <sup>-/-</sup>, and *Ighb*<sup>-/-</sup> mice were purchased from The Jackson Laboratory. Antibiotic-treated mice were fed a cocktail of broad-spectrum antibiotics—namely, ampicillin (1 g/L; Sigma, Bandai, Japan), vancomycin (500 mg/L; Shionogi, Osaka, Japan), neomycin (1 g/L; Sigma), and metronidazole (1 g/L; Sigma)—or were given these antibiotics in their drinking water, for 4 weeks as previously described (48). These mice were maintained in the experimental animal facility at the University of Tokyo. GF and SFB or *L. murinus* gnotobiotic mice (BALB/c) were maintained in the GF animal facility at the Yakult Central Institute and at the University of Tokyo. In all experiments, littermates were used at 6 to 10 weeks of age.

### Isolation of bacterial DNA

The isolation protocol for bacterial DNA was adapted from a previously described method (49), with some modifications. Bacterial samples in the duodenum and ileum were obtained from mice aged 8 weeks. After removal of PPs and intestinal contents, the intestinal tissues were washed three times with phosphate-buffered saline (PBS) for 10 s each time so as to collect bacteria embedded within the intestinal mucus for analysis of microbial composition. These bacteria-containing solutions were centrifuged, and the pellets were suspended in 500  $\mu$ L of TE buffer (10 mM Tris-HCl, 1 mM EDTA; pH 8.0). Glass beads, Tris-phenol buffer, and 10% sodium dodecyl sulfate (SDS) were added to the bacterial suspensions, and the mixtures were vortexed vigorously for 10 s by using a FastPrep FP100 A (BIO 101). After incubation at 65°C for 10 min, the solutions were vortexed and incubated again at 65°C for 10 min. Bacterial DNA was then precipitated in isopropanol, pelleted by centrifugation, washed in 70%

ethanol, and resuspended in TE buffer. Extracted bacterial DNA was subjected to 16S rRNA gene clone library (50).

### 16S rRNA gene clone library analyses

For 16S rRNA gene clone library analyses, bacterial 16S rRNA gene sequences were amplified by means of polymerase chain reaction (PCR) with the 27F (5'-AGAGTTTGATCCTGGCTCAG-3') and 1492R (5'-GGTTACCTTGTACACTT-3') primers. Amplified 16S rDNA was ligated into the pCR4.0 TOPO vector (Invitrogen, Carlsbad, CA), and the products of these ligation reactions were then transformed into DH-5 $\alpha$ -competent cells (TOYOBO, Osaka, Japan). Inserts were amplified and sequenced on an ABI PRISM 3100 Genetic Analyzer (Applied Biosystems, Foster City, CA). The 27F and 520R (5'-ACCGCGGCTGCTGGC-3') primers and a BigDye Terminator cycle sequencing kit (Applied Biosystems) were used for sequencing. Bacterial sequences were identified by means of Basic Local Alignment Search Tool (BLAST) and Ribosomal Database Project searches (50).

### Immunohistochemistry

Immunohistochemical analyses were performed as previously described, with some modifications (51). For whole-mount immunofluorescence staining, the mucus layer was removed by flushing the small intestine with PBS; then, the appropriate parts of the small intestine were fixed with 4% paraformaldehyde for 3 hours. After being washed with PBS, whole-mount tissues were stained for at least 3 hours at 4°C with 20  $\mu$ g/mL UEA-1 conjugated to tetramethylrhodamine B isothiocyanate (UEA-1-TRITC; Vector Laboratories, Burlingame, CA) and 10  $\mu$ g/mL wheat germ agglutinin (WGA) conjugated to Alexa Fluor 633 (Invitrogen). For whole-mount fluorescence in situ hybridization analysis, we modified the protocol previously described (52). After fixation with 4% paraformaldehyde, intestinal tissues were washed with 1 mL PBS and 100  $\mu$ L hybridization buffer (0.9 M NaCl, 20 mM Tris-HCl, 0.1% SDS) containing 2  $\mu$ g EUB338 probe (5'-GCTGCTCCCGTAGGAGT-3') conjugated to Alexa Fluor 488 (Invitrogen). After overnight incubation at 42°C, the tissues were washed with 1 mL PBS and stained for 3 hours with 10  $\mu$ g/mL WGA conjugated to Alexa Fluor 633 in PBS. After being washed with PBS, all tissues were analyzed under a confocal laser-scanning microscope (TCS SP2; Leica Microsystems, Wetzlar, Germany).

### Cell preparations

A standard protocol was used to prepare intestinal ECs (53). Tissues of the small intestine were extensively rinsed with PBS after removal of PPs. After the intestinal contents had been removed, the samples were opened longitudinally and cut into 1-cm pieces. These tissue pieces were mildly shaken in 1 mM EDTA/PBS for 10 min at 37°C. After passage through a 40- $\mu$ m mesh filter, intestinal ECs were resuspended in minimum essential medium containing 20% fetal calf serum (FCS). Lamina propria (LP) cells were collected as previously described (54), with

some modifications. Briefly, isolated small intestine was shaken for 40 min at 37°C in RPMI 1640 containing 10% FCS and 1 mM EDTA. Cell suspensions, including intestinal ECs and intraepithelial lymphocytes, were discarded, and the remaining tissues were further digested with continuous stirring for 60 min at 37°C with 2 mg/mL collagenase (Wako) in RPMI 1640 containing 10% FCS. After passage through a 190- $\mu$ m mesh, the cell suspensions were subjected to Percoll (GE Healthcare) density gradients of 40 and 75%, and the interface between the layers was collected to retrieve LP cells. Stromal cells were identified as CD45<sup>-</sup> Viaprobe<sup>-</sup> cells. For fluorescence-activated cell-sorting (FACS) analysis of ILCs, isolated LP cells were further purified by magnetic-activated cell sorting so as to eliminate CD11b<sup>+</sup>, CD11c<sup>+</sup>, and CD19<sup>+</sup> cells. CD11b<sup>-</sup> CD11c<sup>-</sup> CD19<sup>-</sup> Viaprobe<sup>-</sup> CD45<sup>+</sup> LP cells were used to detect ILCs.

### Antibodies and flow cytometry

For flow cytometric analysis, isolated intestinal ECs were stained with UEA-1-TRITC, anti-CD45-Pacific blue (PB; Biolegend, San Diego, CA), and Viaprobe (BD Biosciences, East Rutherford, NJ). Viaprobe<sup>-</sup> CD45<sup>-</sup> UEA-1<sup>+</sup> cells were identified as F-ECs. After blocking with anti-CD16/32 (Fc $\gamma$ RII/III) (BD Biosciences), the following antibodies were used to stain spleen and LP cells: anti-CD45-PB (Biolegend), anti-CD11b-phycoerythrin (PE), anti-Foxp3-fluorescein isothiocyanate (FITC) (eBioscience, San Diego, CA), anti-CD11c-allophycocyanin (APC), anti-CD11b-FITC, anti-Gr-1-Alexa647, anti-CD3-APC, anti-B220-PE, anti-B220-APC, anti-IgA-FITC, anti-CD4-eFluor450, anti-CD90.2-FITC, anti-IL-17-PE, and anti-IFN $\gamma$ -FITC (all from BD Biosciences), and Viaprobe. CD11b<sup>-</sup> CD11c<sup>-</sup> CD19<sup>-</sup> LP cells were purified by using anti-CD11b, anti-CD11c, and anti-CD19 MicroBeads (Miltenyi Biotec, Bergisch Gladbach, Germany). The results were obtained by using a FACSAria cell sorter (BD Biosciences) with FlowJo software (TreeStar, Ashland, Oregon).

### Intracellular staining of Foxp3 and cytokines

Isolated LP cells were incubated for 4 hours at 37°C with 50 ng/mL phorbol myristate acetate (Sigma), 500 ng/mL ionomycin (Sigma), and GolgiPlug (BD Bioscience) in RPMI 1640 containing 10% FCS and penicillin and streptomycin. After incubation, cells were stained with antibodies against surface antigens for 30 min at 4°C. The cells were fixed and permeabilized with Cytofix/Cytoperm solution (BD Bioscience), and cytokines were stained with the fluorescence-conjugated cytokine antibodies. A Foxp3 staining buffer set (eBioscience) was used for intracellular staining of Foxp3.

### Depletion of CD90<sup>+</sup> ILCs

Depletion of CD90<sup>+</sup> ILCs was performed as previously described, with some modifications (36). Two hundred and fifty micrograms of a mAb to CD90.2 or an isotype control rat IgG2b (BioXCell, West Lebanon, NH) was given by means of intraperitoneal injection a total of three times at

3-day intervals. Intestinal ECs and LP cells were collected 2 days after the final injection.

### Hydrodynamic IL-22 gene delivery system

pLIVE control plasmid (Takara Bio, Shiga, Japan) or IL-22-expressing pLIVE vector (pLIVE-*mIL22*) was introduced into 8-week-old antibiotic-treated C57BL/6 or *Rorc*<sup>sfpr/sfpr</sup> mice. Ten micrograms per mouse of plasmid diluted in ~1.5 mL TransIT-EE Hydrodynamic Delivery Solution (Mirus Bio, Madison, WI) was injected via the tail vein within 7 to 10 s. To assess IL-22 expression, serum IL-22 was quantified by means of an enzyme-linked immunosorbent assay (R&D Systems, Minneapolis, MN).

### Generation of PP-null mice

mAb to IL-7R (A7R34) was kindly provided by S. Nishikawa. PP-null mice were generated by injecting 600 µg of mAb to IL-7R into pregnant mice on embryonic day 14 (55).

### In vivo treatment with LTβR-Ig and antibody to IL-22

Neutralization antibody to IL-22 was purchased from eBioscience. Eight-week-old Rag-deficient mice were injected intraperitoneally with antibody to IL-22 a total of five times at 3-day intervals (on days 0, 3, 6, 9, and 12). Plasmid pMKIT-expressing LTβR-Ig and LTβR-Ig treatment was performed as described previously (56). Four-week-old C57BL/6 mice were injected intraperitoneally once a week for 3 weeks (on days 0, 7, 14, and 21) with LTβR-Ig fusion protein or control human IgG1 at a dose of 50 µg per mouse. Intestinal ECs were analyzed 3 days after the indicated injection time points.

### Adoptive transfer of mixed BM

For mixed BM transfer experiments, *Rorc*<sup>sfpr/sfpr</sup> mice were irradiated with two doses of 550 rad each, 3 hours apart. BM cells ( $1 \times 10^7$ ) from *Rorc*<sup>sfpr/sfpr</sup> mice was mixed with BM cells ( $1 \times 10^7$ ) from C57BL/6 or *Lta*<sup>-/-</sup> mice and intravenously injected into irradiated recipient mice. BM chimeric mice were used for experiments 8 weeks after the BM transfer.

### Isolation of RNA and real-time reverse transcriptase PCR analysis

Intestinal ECs and subsets of LP cells were sorted with a FACSAria cell sorter (BD Biosciences). The sorted cells were lysed in TRIzol reagent (Invitrogen), and total RNA was extracted in accordance with the manufacturer's instructions. RNA was reverse-transcribed by using a SuperScript VILO cDNA Synthesis Kit (Invitrogen). The cDNA was subjected to real-time reverse transcriptase-PCR (rRT-PCR) by using Roche (Basel, Switzerland) universal probe/primer sets specific for *Lta* (primer F: 5'-tcctcagaagcacttgacc-3', R: 5'-gagttctgctgctgggta-3', probe No. 62), *Ltb* (primer F: 5'-cctggtgacactgtgtg-3', R: 5'-tgctctgagccaatgatct-3', probe No. 76), *Il22* (primer F: 5'-ttctgacccaactcagca-3', R: 5'-tctgtagttcttggtgctca-3', probe No. 17), *Il22r1* (primer F: 5'-tgctctgttatctgggctacaa-3', R: 5'-tcagacacgtggacgtt-3', probe No. 9), *Il10rβ* (primer F: 5'-attcggatggatcatg-3', R: 5'-gcatctcaggaggtccatg-

3', probe No. 29), *Fut2* (primer F: 5'-tgactccaccatcc-3', R: 5'-tcgacaggttgagctt-3', probe No. 67), and *Gapdh* (primer F: 5'-tgctcctgctggatctgac-3', R: 5'-cctgctcaccacctcttg-3', probe No. 80). RT-PCR analysis was performed with a Lightcycler II instrument (Roche Diagnostics) to measure the expression levels of specific genes.

### Infection with *S. typhimurium*

Streptomycin-resistant wild-type *S. typhimurium* was isolated from *S. typhimurium* strain ATCC 14028. *Fut2*<sup>-/-</sup> (BALB/c background) and control littermate mice pretreated with 20 mg of streptomycin 24 hours before infection were given  $1 \times 10^8$  colony-forming units of the isolated *S. typhimurium* via oral gavage. After 24 hours, the mice were dissected, and the cecal contents were collected. Isolated cecum was treated with PBS containing 0.1 mg mL<sup>-1</sup> gentamicin at 4°C for 30 min so as to kill bacteria on the tissue surface. The cecum was then homogenized and serial dilutions plated in order to determine the number of *S. typhimurium*. Sections of proximal colon were prepared 48 hours after infection. Infiltration of inflammatory cells was confirmed with hematoxylin and eosin staining.

### Statistical analysis

Statistical analysis was performed with an unpaired, two-tailed Student's *t*-test. *P* values <0.05 were considered statistically significant.

### REFERENCES AND NOTES

- Y. Goto, I. I. Ivanov, Intestinal epithelial cells as mediators of the commensal-host immune crosstalk. *Immunol. Cell Biol.* **91**, 204–214 (2013). doi: 10.1038/icb.2012.80; pmid: 23318659
- J. Qiu et al., Group 3 innate lymphoid cells inhibit T-cell-mediated intestinal inflammation through aryl hydrocarbon receptor signaling and regulation of microflora. *Immunity* **39**, 386–399 (2013). doi: 10.1016/j.immuni.2013.08.002; pmid: 23954130
- S. L. Sanos et al., RORγ<sub>1</sub> and commensal microflora are required for the differentiation of mucosal interleukin 22-producing NKp46<sup>+</sup> cells. *Nat. Immunol.* **10**, 83–91 (2009). doi: 10.1038/ni.1684; pmid: 19029903
- N. Satoh-Takayama et al., Microbial flora drives interleukin 22 production in intestinal NKp46<sup>+</sup> cells that provide innate mucosal immune defense. *Immunity* **29**, 958–970 (2008). doi: 10.1016/j.immuni.2008.11.001; pmid: 19084435
- S. Vaishnava et al., The antibacterial lectin RegIII promotes the spatial segregation of microbiota and host in the intestine. *Science* **334**, 255–258 (2011). doi: 10.1126/science.1209791; pmid: 21998396
- L. Bry, P. G. Falk, T. Midtvedt, J. I. Gordon, A model of host-microbial interactions in an open mammalian ecosystem. *Science* **273**, 1380–1383 (1996). doi: 10.1126/science.273.5280.1380; pmid: 8703071
- L. E. Comstock, D. L. Kasper, Bacterial glycans: Key mediators of diverse host immune responses. *Cell* **126**, 847–850 (2006). doi: 10.1016/j.cell.2006.08.021; pmid: 16959564
- M. J. Coyne, B. Reinap, M. M. Lee, L. E. Comstock, Human symbionts use a host-like pathway for surface fucosylation. *Science* **307**, 1778–1781 (2005). doi: 10.1126/science.1106469; pmid: 15774760
- L. V. Hooper, J. Xu, P. G. Falk, T. Midtvedt, J. I. Gordon, A molecular sensor that allows a gut commensal to control its nutrient foundation in a competitive ecosystem. *Proc. Natl. Acad. Sci. U.S.A.* **96**, 9833–9838 (1999). doi: 10.1073/pnas.96.17.9833; pmid: 10449780
- Y. Goto, H. Kiyono, Epithelial barrier: An interface for the cross-communication between gut flora and immune system. *Immunol. Rev.* **245**, 147–163 (2012). doi: 10.1111/j.1600-065X.2011.01078.x; pmid: 22168418
- K. Terahara et al., Distinct fucosylation of M cells and epithelial cells by Fut1 and Fut2, respectively, in response to intestinal environmental stress. *Biochem. Biophys. Res. Commun.*

- 404, 822–828 (2011). doi: 10.1016/j.bbrc.2010.12.067; pmid: 21172308
- E. A. Hurd, S. E. Domino, Increased susceptibility of secretor factor gene *Fut2*-null mice to experimental vaginal candidiasis. *Infect. Immun.* **72**, 4279–4281 (2004). doi: 10.1128/AI.72.7.4279-4281.2004; pmid: 15213174
- A. Franke et al., Genome-wide meta-analysis increases to 71 the number of confirmed Crohn's disease susceptibility loci. *Nat. Genet.* **42**, 1118–1125 (2010). doi: 10.1038/ng.717; pmid: 21102463
- A. Hazra et al., Common variants of *FUT2* are associated with plasma vitamin B12 levels. *Nat. Genet.* **40**, 1160–1162 (2008). doi: 10.1038/ng.210; pmid: 18776911
- L. Lindesmith et al., Human susceptibility and resistance to Norwalk virus infection. *Nat. Med.* **9**, 548–553 (2003). doi: 10.1038/nm860; pmid: 12692541
- D. P. McGovern et al., International IBD Genetics Consortium, Fucosyltransferase 2 (*FUT2*) non-secretor status is associated with Crohn's disease. *Hum. Mol. Genet.* **19**, 3468–3476 (2010). doi: 10.1093/hmg/ddq248; pmid: 20570966
- D. J. Smyth et al., *FUT2* nonsecretor status links type 1 diabetes susceptibility and resistance to infection. *Diabetes* **60**, 3081–3084 (2011). doi: 10.2337/db11-0638; pmid: 22025780
- B. M. Lambert-Marcille et al., A *FUT2* gene common polymorphism determines resistance to rotavirus A of the P[8] genotype. *J. Infect. Dis.* **209**, 1227–1230 (2014). doi: 10.1093/infdis/jit655; pmid: 24277741
- T. Følseraas et al., Extended analysis of a genome-wide association study in primary sclerosing cholangitis detects multiple novel risk loci. *J. Hepatol.* **57**, 366–375 (2012). doi: 10.1016/j.jhep.2012.03.031; pmid: 22521342
- P. C. Kashyap et al., Genetically dictated change in host mucus carbohydrate landscape exerts a diet-dependent effect on the gut microbiota. *Proc. Natl. Acad. Sci. U.S.A.* **110**, 17059–17064 (2013). doi: 10.1073/pnas.1306070110; pmid: 24062455
- P. Rausch et al., Colonic mucosa-associated microbiota is influenced by an interaction of Crohn disease and *FUT2* (Secretor) genotype. *Proc. Natl. Acad. Sci. U.S.A.* **108**, 19030–19035 (2011). doi: 10.1073/pnas.1106408108; pmid: 22068912
- R. B. Sartor, Microbial influences in inflammatory bowel diseases. *Gastroenterology* **134**, 577–594 (2008). doi: 10.1053/j.gastro.2007.11.059; pmid: 18242222
- J. P. Koopman, A. M. Stadhouders, H. M. Kennis, H. De Boer, The attachment of filamentous segmented micro-organisms to the distal ileum wall of the mouse: A scanning and transmission electron microscopy study. *Lab. Anim.* **21**, 48–52 (1987). doi: 10.1258/002367787780740743; pmid: 3560864
- K. Suzuki et al., Aberrant expansion of segmented filamentous bacteria in IgA-deficient gut. *Proc. Natl. Acad. Sci. U.S.A.* **101**, 1981–1986 (2004). doi: 10.1073/pnas.0307317101; pmid: 14766966
- V. Gaboriau-Routhiau et al., The key role of segmented filamentous bacteria in the coordinated maturation of gut helper T cell responses. *Immunity* **31**, 677–689 (2009). doi: 10.1016/j.immuni.2009.08.020; pmid: 19833089
- I. I. Ivanov et al., Induction of intestinal Th17 cells by segmented filamentous bacteria. *Cell* **139**, 485–498 (2009). doi: 10.1016/j.cell.2009.09.033; pmid: 19836068
- I. I. Ivanov et al., Specific microbiota direct the differentiation of IL-17-producing T-helper cells in the mucosa of the small intestine. *Cell Host Microbe* **4**, 337–349 (2008). doi: 10.1016/j.chom.2008.09.009; pmid: 18854238
- C. P. Davis, D. C. Savage, Habitat, succession, attachment, and morphology of segmented, filamentous microbes indigenous to the murine gastrointestinal tract. *Infect. Immun.* **10**, 948–956 (1974). pmid: 4426712
- Y. Umesaki, H. Setoyama, S. Matsumoto, A. Imaoka, K. Itoh, Differential roles of segmented filamentous bacteria and clostridia in development of the intestinal immune system. *Infect. Immun.* **67**, 3504–3511 (1999). pmid: 10377132
- I. I. Ivanov et al., The orphan nuclear receptor RORγ<sub>1</sub> directs the differentiation program of proinflammatory IL-17<sup>+</sup> T helper cells. *Cell* **126**, 1121–1133 (2006). doi: 10.1016/j.cell.2006.07.035; pmid: 16990136
- H. Spits et al., Innate lymphoid cells—A proposal for uniform nomenclature. *Nat. Rev. Immunol.* **13**, 145–149 (2013). doi: 10.1038/nri3365; pmid: 23348417
- H. Spits, J. P. Di Santo, The expanding family of innate lymphoid cells: Regulators and effectors of immunity and tissue remodeling. *Nat. Immunol.* **12**, 21–27 (2011). doi: 10.1038/ni.1962; pmid: 21113163

33. Y. Yokota *et al.*, Development of peripheral lymphoid organs and natural killer cells depends on the helix-loop-helix inhibitor Id2. *Nature* **397**, 702–706 (1999). doi: [10.1038/17812](https://doi.org/10.1038/17812); pmid: [10067894](https://pubmed.ncbi.nlm.nih.gov/10067894/)
34. G. Eberl *et al.*, An essential function for the nuclear receptor ROR $\gamma$ (t) in the generation of fetal lymphoid tissue inducer cells. *Nat. Immunol.* **5**, 64–73 (2004). doi: [10.1038/ni1022](https://doi.org/10.1038/ni1022); pmid: [14691482](https://pubmed.ncbi.nlm.nih.gov/14691482/)
35. S. Sawa *et al.*, ROR $\gamma$ t<sup>+</sup> innate lymphoid cells regulate intestinal homeostasis by integrating negative signals from the symbiotic microbiota. *Nat. Immunol.* **12**, 320–326 (2011). doi: [10.1038/ni.2002](https://doi.org/10.1038/ni.2002); pmid: [21336274](https://pubmed.ncbi.nlm.nih.gov/21336274/)
36. G. F. Sonnenberg, L. A. Monticelli, M. M. Elloso, L. A. Fouser, D. Artis, CD4(+) lymphoid tissue-inducer cells promote innate immunity in the gut. *Immunity* **34**, 122–134 (2011). doi: [10.1016/j.immuni.2010.12.009](https://doi.org/10.1016/j.immuni.2010.12.009); pmid: [21194981](https://pubmed.ncbi.nlm.nih.gov/21194981/)
37. S. Buonocore *et al.*, Innate lymphoid cells drive interleukin-23-dependent innate intestinal pathology. *Nature* **464**, 1371–1375 (2010). doi: [10.1038/nature08949](https://doi.org/10.1038/nature08949); pmid: [20393462](https://pubmed.ncbi.nlm.nih.gov/20393462/)
38. G. Pickert *et al.*, STAT3 links IL-22 signaling in intestinal epithelial cells to mucosal wound healing. *J. Exp. Med.* **206**, 1465–1472 (2009). doi: [10.1084/jem.20082683](https://doi.org/10.1084/jem.20082683); pmid: [19564350](https://pubmed.ncbi.nlm.nih.gov/19564350/)
39. G. F. Sonnenberg, L. A. Fouser, D. Artis, Functional biology of the IL-22-IL-22R pathway in regulating immunity and inflammation at barrier surfaces. *Adv. Immunol.* **107**, 1–29 (2010). doi: [10.1016/B978-0-12-381300-8.00001-0](https://doi.org/10.1016/B978-0-12-381300-8.00001-0); pmid: [21034969](https://pubmed.ncbi.nlm.nih.gov/21034969/)
40. M. Tsuji *et al.*, Requirement for lymphoid tissue-inducer cells in isolated follicle formation and T cell-independent immunoglobulin A generation in the gut. *Immunity* **29**, 261–271 (2008). doi: [10.1016/j.immuni.2008.05.014](https://doi.org/10.1016/j.immuni.2008.05.014); pmid: [18656387](https://pubmed.ncbi.nlm.nih.gov/18656387/)
41. P. De Togni *et al.*, Abnormal development of peripheral lymphoid organs in mice deficient in lymphotoxin. *Science* **264**, 703–707 (1994). doi: [10.1126/science.8171322](https://doi.org/10.1126/science.8171322); pmid: [8171322](https://pubmed.ncbi.nlm.nih.gov/8171322/)
42. D. Chessa, M. G. Winter, M. Jakomin, A. J. Bäuml, *Salmonella enterica* serotype Typhimurium Std fimbriae bind terminal  $\alpha$  (1,2)fucose residues in the cecal mucosa. *Mol. Microbiol.* **71**, 864–875 (2009). doi: [10.1111/j.1365-2958.2008.06566.x](https://doi.org/10.1111/j.1365-2958.2008.06566.x); pmid: [19183274](https://pubmed.ncbi.nlm.nih.gov/19183274/)
43. M. Awoniyi, S. I. Miller, C. B. Wilson, A. M. Hajjar, K. D. Smith, Homeostatic regulation of *Salmonella*-induced mucosal inflammation and injury by IL-23. *PLOS One* **7**, e37311 (2012). doi: [10.1371/journal.pone.0037311](https://doi.org/10.1371/journal.pone.0037311); pmid: [22624013](https://pubmed.ncbi.nlm.nih.gov/22624013/)
44. I. Godínez *et al.*, T cells help to amplify inflammatory responses induced by *Salmonella enterica* serotype Typhimurium in the intestinal mucosa. *Infect. Immun.* **76**, 2008–2017 (2008). doi: [10.1128/IAI.01691-07](https://doi.org/10.1128/IAI.01691-07); pmid: [18347048](https://pubmed.ncbi.nlm.nih.gov/18347048/)
45. A. V. Tumanov *et al.*, Lymphotoxin controls the IL-22 protection pathway in gut innate lymphoid cells during mucosal pathogen challenge. *Cell Host Microbe* **10**, 44–53 (2011). doi: [10.1016/j.chom.2011.06.002](https://doi.org/10.1016/j.chom.2011.06.002); pmid: [21767811](https://pubmed.ncbi.nlm.nih.gov/21767811/)
46. S. E. Domino, L. Zhang, P. J. Gillespie, T. L. Saunders, J. B. Lowe, Deficiency of reproductive tract  $\alpha$ (1,2)fucosylated glycans and normal fertility in mice with targeted deletions of the FUT1 or FUT2  $\alpha$ (1,2)fucosyltransferase locus. *Mol. Cell. Biol.* **21**, 8336–8345 (2001). doi: [10.1128/MCB.21.24.8336-8345.2001](https://doi.org/10.1128/MCB.21.24.8336-8345.2001); pmid: [11713270](https://pubmed.ncbi.nlm.nih.gov/11713270/)
47. K. Kreymborg *et al.*, IL-22 is expressed by Th17 cells in an IL-23-dependent fashion, but not required for the development of autoimmune encephalomyelitis. *J. Immunol.* **179**, 8098–8104 (2007). doi: [10.4049/jimmunol.179.12.8098](https://doi.org/10.4049/jimmunol.179.12.8098); pmid: [18056351](https://pubmed.ncbi.nlm.nih.gov/18056351/)
48. S. Rakoff-Nahoum, J. Paglino, F. Eslami-Varzaneh, S. Edberg, R. Medzhitov, Recognition of commensal microflora by toll-like receptors is required for intestinal homeostasis. *Cell* **118**, 229–241 (2004). doi: [10.1016/j.cell.2004.07.002](https://doi.org/10.1016/j.cell.2004.07.002); pmid: [15260992](https://pubmed.ncbi.nlm.nih.gov/15260992/)
49. T. Matsuki *et al.*, Quantitative PCR with 16S rRNA-gene-targeted species-specific primers for analysis of human intestinal bifidobacteria. *Appl. Environ. Microbiol.* **70**, 167–173 (2004). doi: [10.1128/AEM.70.1.167-173.2004](https://doi.org/10.1128/AEM.70.1.167-173.2004); pmid: [14711639](https://pubmed.ncbi.nlm.nih.gov/14711639/)
50. R. Kibe, M. Sakamoto, H. Hayashi, H. Yokota, Y. Benno, Maturation of the murine cecal microbiota as revealed by terminal restriction fragment length polymorphism and 16S rRNA gene clone libraries. *FEMS Microbiol. Lett.* **235**, 139–146 (2004). doi: [10.1111/j.1574-6968.2004.tb09578.x](https://doi.org/10.1111/j.1574-6968.2004.tb09578.x); pmid: [15158273](https://pubmed.ncbi.nlm.nih.gov/15158273/)
51. M. H. Jang *et al.*, Intestinal villous M cells: An antigen entry site in the mucosal epithelium. *Proc. Natl. Acad. Sci. U.S.A.* **101**, 6110–6115 (2004). doi: [10.1073/pnas.0400969101](https://doi.org/10.1073/pnas.0400969101); pmid: [15071180](https://pubmed.ncbi.nlm.nih.gov/15071180/)
52. T. Obata *et al.*, Indigenous opportunistic bacteria inhabit mammalian gut-associated lymphoid tissues and share a mucosal antibody-mediated symbiosis. *Proc. Natl. Acad. Sci. U.S.A.* **107**, 7419–7424 (2010). doi: [10.1073/pnas.1001061107](https://doi.org/10.1073/pnas.1001061107); pmid: [20360558](https://pubmed.ncbi.nlm.nih.gov/20360558/)
53. M. Yamamoto, K. Fujihashi, K. Kawabata, J. R. McGhee, H. Kiyono, A mucosal intranet: Intestinal epithelial cells down-regulate intraepithelial, but not peripheral, T lymphocytes. *J. Immunol.* **160**, 2188–2196 (1998). ; pmid: [9498757](https://pubmed.ncbi.nlm.nih.gov/9498757/)
54. N. Ohta *et al.*, IL-15-dependent activation-induced cell death-resistant Th1 type CD8  $\alpha$   $\beta$  NK1.1<sup>+</sup> T cells for the development of small intestinal inflammation. *J. Immunol.* **169**, 460–468 (2002). doi: [10.4049/jimmunol.169.1.460](https://doi.org/10.4049/jimmunol.169.1.460); pmid: [12077277](https://pubmed.ncbi.nlm.nih.gov/12077277/)
55. H. Yoshida *et al.*, IL-7 receptor  $\alpha$ <sup>+</sup> CD3(-) cells in the embryonic intestine induces the organizing center of Peyer's patches. *Int. Immunol.* **11**, 643–655 (1999). doi: [10.1093/intimm/11.5.643](https://doi.org/10.1093/intimm/11.5.643); pmid: [10330270](https://pubmed.ncbi.nlm.nih.gov/10330270/)
56. M. Yamamoto *et al.*, Role of gut-associated lymphoreticular tissues in antigen-specific intestinal IgA immunity. *J. Immunol.* **173**, 762–769 (2004). doi: [10.4049/jimmunol.173.2.762](https://doi.org/10.4049/jimmunol.173.2.762); pmid: [15240662](https://pubmed.ncbi.nlm.nih.gov/15240662/)

## ACKNOWLEDGMENTS

We thank M. Shimaoka, G. Eberl, M. Pasparakis, K. Honda, C. A. Hunter, C. O. Elson, and J. R. Mora for their critical and helpful comments and advice on this research. Y. Yokota and M. Yamamoto kindly provided Id2-deficient mice and LT $\beta$ R-Ig, respectively. R. Curtis III and H. Matsui kindly provided several strains of *Salmonella typhimurium*. We thank Y. Akiyama for her technical support with the *S. typhimurium* infection model. S. Tanaka gave us helpful technical suggestions for performing flow cytometric analysis. The data presented in this paper are tabulated in the main paper and in the supplementary materials. Sequences of the bacterial 16S rRNA genes obtained from duodenal and ileal mucus bacteria have been deposited in the International Nucleotide Sequence Database (accession nos. AB470733 to AB470815). This work was supported by grants from the following sources: the Core Research for Evolutional Science and Technology Program of the Japan Science and Technology Agency (to H.K.); a Grant-in-Aid for Scientific Research on Priority Areas, Scientific Research (S) (to H.K.); Specially Promoted Research (230000-12 to C.S.); Scientific Research (B) (to J.K.); for the Leading-edge Research Infrastructure Program and the Young Researcher Overseas Visits Program for Vitalizing Brain Circulation (to Y.G., J.K., and H.K.); for the Leading-edge Research Infrastructure Program (to J.K. and H.K.) from the Ministry of Education, Culture, Sports, Science and Technology of Japan; the Global Center of Excellence (COE) Program "Center of Education and Research for Advanced Genome-based Medicine" (to H.K.); the Ministry of Health, Labor and Welfare of Japan (to J.K. and H.K.); the Science and Technology Research Promotion Program for Agriculture, Forestry, Fisheries and Food Industry (to J.K.); Mochida Memorial Foundation for Medical and Pharmaceutical Research (to J.K.); the National Institutes of Health (1R01DK098378 to I.I.); and by the Crohn's and Colitis Foundation of America (SRA#259540 to I.I.). The authors declare no conflicts of interest.

## SUPPLEMENTARY MATERIALS

[www.sciencemag.org/content/345/6202/1254009/suppl/DC1](http://www.sciencemag.org/content/345/6202/1254009/suppl/DC1)  
Figs. S1 to S11  
Table S1

27 March 2014; accepted 25 July 2014  
[10.1126/science.1254009](https://doi.org/10.1126/science.1254009)